Bending Behavior of Flexible Crystalline Silicon Nanomembrane Photonic Crystal Microcavities

Xiaochuan Xu[1,2,*], Harish Subbaraman[2,*], Swapnajit Chakravarty[2], and Ray T. Chen[1]
[1]*The University of Texas at Austin – 10100 Burnet Rd, PRC/MER 160, Austin, TX 78758 (USA)*
[2]*Omega Optics, Inc – 10306 Sausalito Dr, Austin, TX 78731 (USA)*
**authors contribute equally*
Author e-mail address: (xiaochuan.xu@utexas.edu, raychen@uts.cc.utexas.edu)

Abstract: We demonstrated a flexible crystalline silicon nanomembrane photonic crystal microcavity with a quality factor of 22,000 and experimentally studied its bending behavior.
OCIS codes: (350.4238) Nanophotonics and photonic crystals; (310.6628) Subwavelength Structures, Nanostructuresl

Flexible and conformal electronic devices promise tremendous applications in areas such as wearable and biomedical electronics [1], which are unthinkable using conventional material systems. Benefits on a similar scale are also foreseeable for photonic devices. However, the difficulty in transferring intricate photonic devices, has deterred widespread developmental activities. The performance of photonic devices heavily relies on the integrity of the geometry, and the tolerance is astonishingly low. The "peel" and "stamp" operations, which are essentials of the conventional stamp printing process, unfortunately can potentially produce geometrical imperfections. In this paper, we present a transfer method which could reliably transfer photonic devices on to flexible substrates. With this method, we transferred a flexible L13 photonic crystal cavity and studied its bending behavior both experimentally and theoretically.

Fig. 1a shows the transferred 2 cm × 2 cm silicon nanomembrane and the transfer process (inset). The photonic devices are patterned on a 2 cm ×2 cm silicon-on-insulator (Soitec SOI) chip with a 250 nm single crystal silicon layer, 3 μm buried oxide layer (BOX), and a 675 μm silicon handle using electron beam lithography (EBL) and reactive ion etching (RIE, HBr/Cl_2) (Fig.1a, inset 1). The patterned chip is flipped over and bonded onto a 125 μm thick polyimide substrate (Dupont™ Kapton® HN) through adhesive bonding with SU-8 (Microchem) (Fig.1a, inset 2). The native oxide on the SOI chip is removed by 1:6 buffered oxide etchant (BOE) prior to bonding because the adhesion between SU-8 and SiO_2 is weak. Prior to bonding, the polyimide film is mounted on a rigid substrate. SU-8 is spin coated on both the polyimide film and the SOI chip, both of which are baked at 65 °C for an extended period of time to improve surface quality as SU-8 has impressive self-planarization capability when heated above its glass transition temperature [2]. The SU-8 layer on the polyimide film is partially exposed to generate Lewis acid, which initiates crosslinking when the unexposed SU-8 on SOI is brought in contact. The pressure is applied by a home-made bonder. After bonding, the silicon handle is removed by mechanical polishing followed by deep reactive ion etching (DRIE), as shown in Fig. 1c. The etch rate is about 2.7 μm/cycle with a selectivity of 80:1 to silicon dioxide (SiO_2), making the 3 μm thick BOX an excellent etch stop layer, which is then removed by concentrated 49% hydrofluoric acid (HF) (Fig.1a, inset 3). Finally, the polyimide film containing the silicon nanomembrane devices is peeled up from the rigid carrier (Fig.1a, inset 4). Fig.1b and c show the scanning electron microscope (SEM) images of the transferred L13 photonic crystal microcavity (and the subwavelength grating (SWG) couplers, respectively. The cavity shows a quality factor of 22000 with glycerol (~9000 with water) as the top cladding,

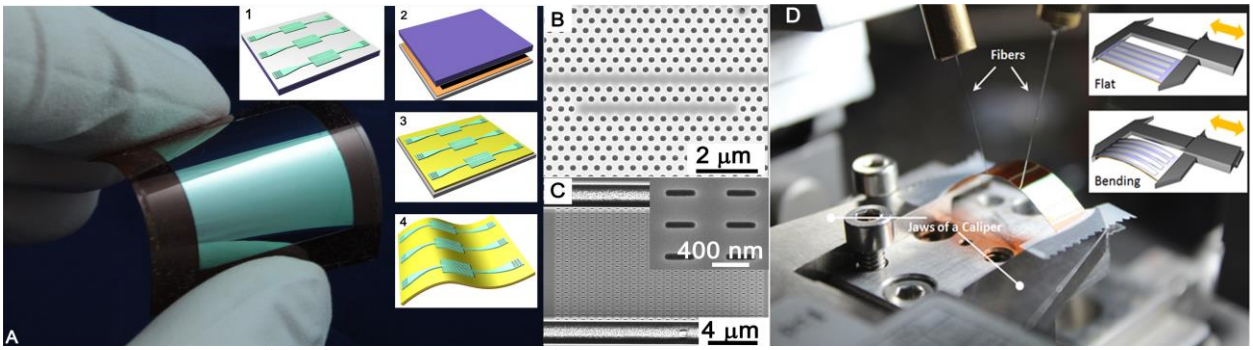

Fig. 1. (a) The optical image of transferred sample. Inset: Transfer process. (1) Pattern the photonic crystal microcavity on SOI. (2) Flip bond the SOI chip on to the Kapton film with SU-8 epoxy. (3) Remove the handle and BOX layer with mechanic polishing, DRIE, and wet etching. (4) Peel off the Kapton film from the mechanic support. SEM images of (b) L13 cavity and (c) grating coupler. (d) Configuration of the bending experiment. Inset: sliding the movable jaws will buckle the specimen upwards or downwards.

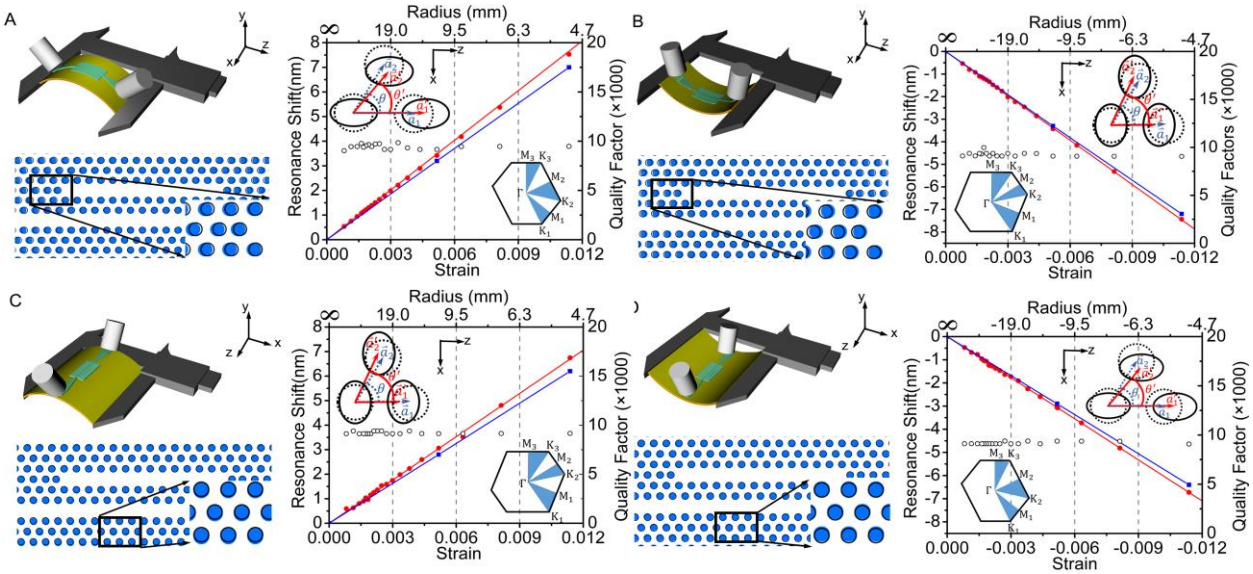

Fig. 2. The bending characteristics of the transferred L13 PC microcavity under (A) LFO bending, (B) LFI bending, (C) TFO bending, and (D) TFI bending. The top left insets are the schematics depicting the bending configurations. The bottom left insets show the deformed geometries generated by FEM simulations. The right figures show the experimental (red) and simulation (blue) correlation between resonance wavelength shift and strain. The insets in the right figures show the deformation of the holes and the corresponding distortion of the reciprocal lattice. The small black circles are the measured quality factors of the cavity at different bending radii.

The bending behavior of the L13 microcavity are investigated with the measurement set-up shown in Fig.1d. The two ends of the sample are constrained on the jaws of a caliper, but allowed to rotate freely. The specimen is buckled upwards or downwards by sliding the movable jaw inwards. The system allows the distance between the two jaws to be controlled with an accuracy better than 0.1 mm. Light is coupled *via* single mode fibers into and out of the device through SWGs [3]. The bending shape of the specimen can be approximated by a sinusoidal function[4]. The bending radius at the peak of the curvature is estimated by the second derivative of the sinusoidal curve. We investigated four different types of axial bending: longitudinal face-out bending (LFO), longitudinal face-in bending (LFI), transverse face-out bending (TFO), and transverse face-in bending (TFI). For longitudinal bending, the bending direction is parallel to the light propagation direction (z axis), while it is perpendicular for transverse bending (x axis). In face-out bending (bending radius R>0), the silicon nanomembrane experiences tensile stress in the bending direction, and in face-in bending (R<0), it experiences compressive stress in the bending direction. The strain γ_{bend} of the silicon nanomembrane in the bending direction equals the distance from the neutral surface, d_n, divided by the bending radius R [4]. The absolute value of R is between infinity (flat) and 5 mm. The corresponding absolute value of the strain $|\gamma_{bend}|$ in the bending direction is between 0 and 1.2%. The experimentally observed shifts of resonance in LFO, LFI, TFO, and TFI bending are shown by the red dots in Fig. 2a-d, respectively. The resonance shifts to longer wavelength when the specimen is under tensile strain ($\gamma_{bend} > 0$), and to shorter wavelength when it is under compressive strain ($\gamma_{bend} < 0$).The resonant shift exhibits a linear correlation with strain. The sensitivities for LFO, LFI, TFO, and TFI are 0.673 pm/με, 0.656 pm/με, 0.588 pm/με, and 0.591 pm/με, respectively, as calculated by linear regression. The 2D simulation with finite element method (FEM) and finite difference time domain (FDTD) shows a good match with the experimental results. The quality factor stays constant for different bending radius as shown by the circles in Fig. 2.

In conclusion, we demonstrated a flexible single crystal silicon nanomembrane photonic crystal microcavity and investigated its mechanic properties. It could be used to monitor the mechanic behavior of aircraft, human joints, etc.

This research was funded by the AirForce Office of Scientific Research (AFOSR) Multidisciplinary University Research Initiative (MURI) under contract No. FA9550-08-1-0394 and Small Business Technology Transfer (STTR) under contract No. FA9550-11-C-0014 (program manager: Dr. G. Pomrenke).

References

[1] J.A. Rogers, et al., "Synthesis, assembly and applications of semiconductor nanomembranes," Nature **477**, 45-53 (2011)
[2] S. Keller, et al.,"Processing of thin SU-8 films," J. Micromech. Microeng. **18**, 125020 (2008)
[3] X. Xu, et al., "Complementary metal–oxide–semiconductor compatible high efficiency subwavelengthgrating couplers for silicon integrated photonics," Appl. Phys. Lett. **101**, 031109 (2012)
[4] S. L. Park, et al., "Theoretical and experimental studies of bending of inorganic electronic materials on plastic substrates," Adv. Funct. Mater. **18**, 2673-2684 (2008)